Thermal and optical simulation of InP on Si nanocavity lasers

P. Wen, P. Tiwari, K. E. Moselund and B. Gotsmann.

IBM Research Europe, Säumerstrasse 4, 8803 Rüschlikon, Switzerland (e-mail: pew@zurich.ibm.com).

***Abstract*—Accurate prediction of thermal effects is important for scaled photonic devices as excessive heating may lead to device failure. This paper addresses numerical modeling of thermal properties of InP nanocavity lasers on Si combined with optical simulations in Lumerical and lasing threshold measurements. Different geometries with diameters ranging from 200 nm to 2 µm are studied, revealing an optimal diameter of around 1000 nm when considering both thermal effects and optical confinement. The temperature profile of the nanocavity lasers reveals that thinning the underlying SiO_2 is the most efficient way to improve the thermal properties of the nanocavity lasers.**

I. Introduction

Semiconductor nanocavity lasers are excellent candidates for light sources due to their low-loss whispering gallery modes, high quality factor and low power consumption [1-3]. III-V on silicon nanocavity lasers in telecommunication wavelengths are the most promising candidates for on-chip light sources. Nanocavity lasers with various geometries and diameters have been demonstrated using optical or electrical pumping [4-7]. However, the serious self-heating problem is an obstacle towards high performance nanocavity lasers, especially when they are integrated with other components. Due to the small volume, the power density in the nanocavity lasers is high, while the buried oxide with low thermal conductivity makes the heat generated by the nanocavity lasers difficult to dissipate through the silicon substrate. In [8] numerical and experimental analysis of microdisk lasers on Si were carried out, revealing high thermal resistance of around 10 K/mW (10^3K/W), and an optimized structure of microdisks with a heatsink in the center region was demonstrated later with thermal resistance reduction of 64% [9]. However, this is still extremely high compared with ridge lasers which show a thermal resistance level of several tens of K/W [10]. Until now there is no systematic analysis on the thermal design of nanocavity lasers considering both geometries and diameters of the microcavities.

In this paper, we present a combined thermal and optical analysis of InP nanocavity lasers using numerical modeling with both Ansys APDL and Lumerical FDTD. Different geometries of disk, square, hexagon and ring structures are studied with various diameters from 200 nm to 2 µm, giving an optimal diameter of around 1000 nm. Temperature profiles in different parts of the nanocavity lasers are studied, revealing that reducing the thickness of the SiO_2 is the most efficient way to improve the thermal property of the nanocavity lasers.

II. Models and parameters

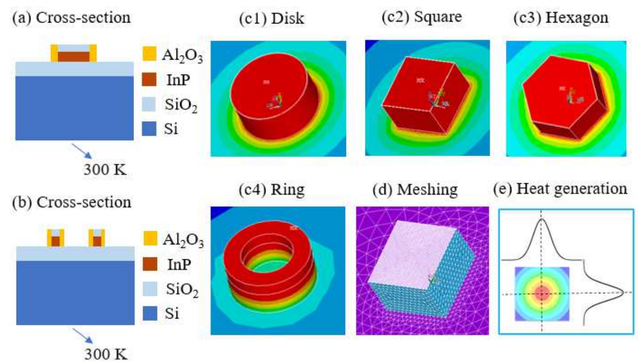

Fig. 1. The Schematic configuration (a) cross-section of (c1) disk (c2) square (c3) hexagon; (b) cross-section of (c4) ring; (d) meshing of square model; (e) gaussian distributed heat generation on square model. The thermal conductivity used in the simulation for Si, SiO_2, InP and Al_2O_3 is 131 W/m·K, 1.4 W/m·K, 68 W/m·K and 35 W/m·K, respectively.

Finite-element analysis (FEA) is used for thermal simulation. Fig. 1 shows the models used in the simulation with underlying SiO_2 thickness of 2 µm and Al_2O_3 thickness of 5 nm. The temperature of the backside of the Si substrate is set to 300 K. A gaussian distributed heat generation incident on the microcavity is used as shown in Fig. 1(e), modeling a laser injection with spot size of 1 µm and total heat of 1.69 mW, corresponding to experimental conditions in our micro-photoluminescence characterization setup. Considering that the lasers are measured inside a cryostat with fixed temperature, heat convection is neglected in the simulation. The heat transfer of the microcavity lasers is modeled using Fourier's law of heat conduction ($q = -\kappa \cdot \nabla T$) to calculate the heat flow [11], where q is the local heat flux density, κ is the thermal conductivity and ∇T is the local temperature gradient.

III. Results and discussion

Fig. 2(a) shows the thermal resistance of the disk, square and hexagon microcavity dependent on the diameter. As the diameter D of each geometry increases, the thermal resistance decreases dramatically, but will finally tend to a saturation value around 200 K/mW. When we compare the same diameter with different geometries, the disks show the lowest thermal resistance. Including thermal boundary conductance (TBC) between InP and SiO_2 (10^8 W/m^2·K) only changes the results marginally for smaller diameters (Fig. 2a) However, the thermal resistance of the microdisk is clearly dominated by the

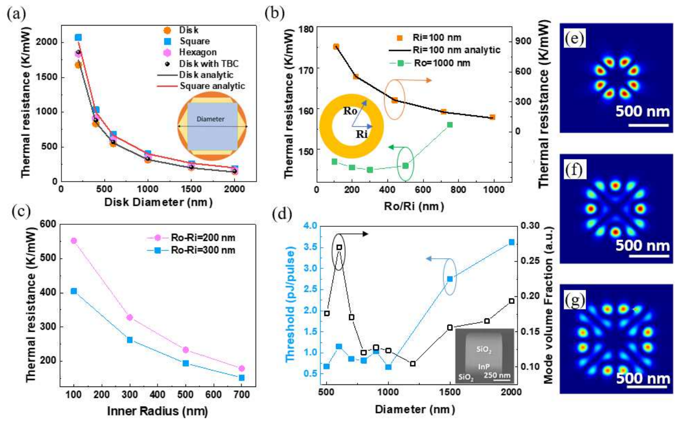

Fig. 2(a)Thermal resistance of disk, square and hexagon microcavity dependent on diameter; (b) and (c) thermal resistance of ring cavities dependent on ring parameter, (d) Experimental threshold versus diameter of InP whispering gallery mode cavities and simulated mode volume fractions. (e)-(g) Simulated resonant modes corresponding to the mode volumes in (d) with diameters of 500 nm, 700 nm, 900 nm.

thermal spreading resistance into the Si/SiO_2 substrate, the FEA results are well approximated using the thermal spreading resistance ($(2\kappa D)^{-1}$) with the well-known correction for finite film thickness (shown by the analytic lines in Fig. 2 (a)). Fig. 2(b) shows the thermal resistance of the micro-ring cavities dependent on the ring diameter. The orange squares show the thermal resistance of the micro-ring cavity with a fixed inner radius of 100 nm, which indicates a dramatic decrease of thermal resistance from 830 K/mW to 150 K/mW as the outer radius increase from 200 nm to 1000 nm. However, when we fix the outer radius to 1000 nm, the thermal resistance shows a similar value of around 150 K/mW (with a minimum of 145 K/mW at 300 nm). We also plotted the thermal resistance versus area which shows similar trend. The plots versus radius are shown here to have an intuitive comparison with the optical simulation. We calculated the thermal resistance of a ring cavity with constant outer and inner radius difference, as shown in Fig. 2 (c). The wider ring always shows lower thermal resistance. Again, the thermal resistance is governed by the thermal spreading resistance into the substrate. Notably, the same fit as used above $(2\kappa D)^{-1}$ with thin film correction describes the data well when using the outer radius, despite the finite inner radius ring. We can conclude that in order to reduce thermal resistance, one needs to increase the outer radius, reduce the oxide film thickness, or replace the SiO_2 with a better thermal conductor.

Fig. 2(d) shows the experimental results characterized in [6] and alongside simulated mode volume fractions occupying the cavity volume and their corresponding simulated resonant mode patterns obtained via 3D finite differences time domain simulations. The smallest cavities have a higher mode volume fraction and high radiation losses, which decrease upon increasing diameter. Beyond diameters of ~1200 nm the volume fraction increases again, likely due to different resonant modes which do not only propagate at the periphery of the cavity. At the same time the threshold increases as well. The cavities are excited with a small excitation spot (1 µm) in the middle of the device. For the devices smaller than 1000 nm the pumping will remain approximately uniform across the area. For the bigger cavities with diameters exceeding the spot size,

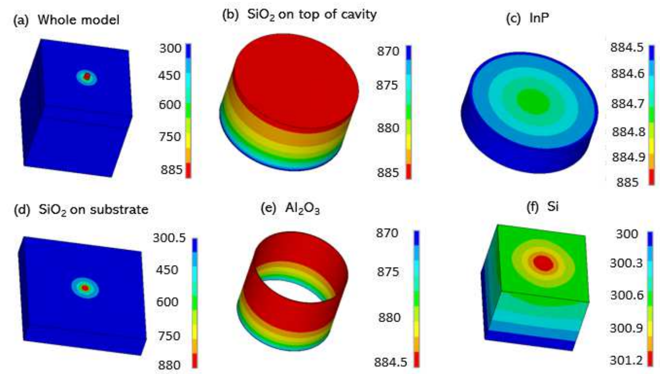

Fig. 3. Temperature profile of the micro-disk laser with diameter of 600 nm.

pumping becomes less efficient with the 1 µm spot size resulting in higher thresholds. For practical applications, cavities with diameters of around 1000 nm are optimal considering the trade-off between uniform pumping conditions in our setup and the thermal resistance.

Fig. 3 shows the temperature profile of different parts of the microdisk laser, (a) to (f) show the temperature profile of the whole structure, SiO_2 on top of cavity, InP, SiO_2 on substrate Al_2O_3, and the Si substrate. Comparing the temperature variation in each part, one can see that the largest temperature difference locates in the SiO_2 on substrate, in agreement with the interpretation above. This indicates that reducing the SiO_2 thickness on substrate could help decrease the thermal resistance efficiently. But an optimal SiO_2 thickness should also consider the leakage of the optical mode into the substrate.

Acknowledgements

This work received financial support from European Union H2020 ERC StG PLASMIC, grant #678567 and H2020 MSCA IF project DATENE, grant #844541.

References

[1] A. B. Matsko, et al., IEEE J. of Sel. Top. In Quantum Electronics, vol. 12, no. 1, pp. 1-14, 2006.
[2] K. Djordjev, et al., IEEE Photonics Technology Letters 14(3), pp. 331-333, 2002.
[3] H. Yoshioka, et al., Scientific Reports 5, no. 10623, 2015.
[4] F. Yuanlong, et al., IEEE J. of Quantum Electronics, vol. 54, no. 5, 2018.
[5] S. Zhu et al., Optics Lett. vol. 44, no. 18, 2019.
[6] P. Tiwari, et al., Optics Express. vol. 29, no. 3, 2021.
[7] C. Lee, et al., IEEE Photonics Technology Letters. vol. 26, no. 15, 2014.
[8] J. Campenhout, et al., Journal of Lightwave Technology, vol. 25, no. 6, 2007.
[9] Z. Wang, et al., Opt Quant Electron. vol. 57, pp. 453-461, 2015.
[10] E. Alkhazraji, et al., Optics and Laser Technology. vol. 98, pp. 67-74, 2018.
[11] M. Wang, et al., FHMT, vol. 1, no. 013004, 2010.